doi:10.1006/jmbi.2001.4994 available online at http://www.idealibrary.com on IDEAL® *J. Mol. Biol.* (2001) **312**, 1037–1049

JMB

Intrinsic Bending and Deformability at the T-A Step of CCTTTAAAGG: A Comparative Analysis of T-A and A-T Steps within A-tracts

Darcy R. Mack[1], Thang K. Chiu[1,3] and Richard E. Dickerson[1,2]*

[1]*Department of Chemistry and Biochemistry, University of California, Los Angeles CA 90095, USA*

[2]*Molecular Biology Institute University of California, Los Angeles, CA 90095, USA*

[3]*Laboratory of Molecular Biology, NIDDK, NIH Building 5, Room 335 Bethesda, MD 20892, USA*

**Corresponding author*

Introduction of a T-A or pyrimidine-purine step into a straight and rigid A-tract can cause a positive roll deformation that kinks the DNA helix at that step. In CCTTTAAAGG, the central T-A step has an 8.6° bend toward the major groove. We report the structural analysis of CCTTTAAAGG and a comparison with 25 other representative crystal structures from the NDB containing at least four consecutive A or T bases. On average, more local bending occurs at the disruptive T-A step (8.21°) than at an A-T step (5.71°). In addition, A-tracts containing an A-T step are more bent than are pure A-tracts, and hence A-A and A-T steps are not equivalent. All T-A steps examined exhibit positive roll, bending towards the major groove, while A-T steps display negative roll and bend slightly towards the minor groove. This illustrates how inherent negative and positive roll are, respectively, at A-T and T-A steps within A-tracts. T-A steps are more deformable, showing larger and more variable deformations of minor groove width, rise, cup, twist, and buckle. Standard deviations of twist, rise, and cup for T-A steps are 6.66°, 0.55 Å, and 15.90°, *versus* 2.28°, 0.21 Å, and 2.99° for A-T steps. Packing constraints determine which local values of these helical parameters an individual T-A step will adopt. For instance, with CCTTTAAAGG and three isomorphous structures, CGATTAATCG, CGATATATCG, and CGATCGATCG, crystal packing forces lead to a series of correlated changes: widened minor groove, large slide, low twist, and large rise. The difference in helical parameters between A-T steps lying within A-tracts, *versus* A-T steps within alternating AT sequences, demonstrates the importance of neighboring steps on the conformation of a given dinucleotide step.

Keywords: A-tract bending; T-A *versus* A-T steps; structural deformability; sequence-structure relationships; DNA conformation

Introduction

Understanding A-tracts is critical to deciphering interactions of DNA with proteins and drugs because A-A steps are the most prevalent of all dinucleotide steps in protein-DNA complexes. Moreover, fully one-third of the dinucleotides in structures published before 1998 are AA, AT, or T-A steps.[1] Previous crystal structures of native DNA and DNA/protein complexes have shown that A-tracts containing at least four consecutive As or Ts, without a disruptive T-A step, are relatively straight and rigid with a deep and narrow minor groove and very small roll and slide deformations.[2–10] Pure A-tracts are resistant to roll bending because the base-pairs are highly propeller-twisted and interlocked by hydrogen bonds. An A-tract containing an A-T step also is straight because the thymine methyl group clashes sterically with the sugar/phospate backbone, blocking roll compression towards the major groove and inducing large propeller twist angles.[11]

A pyrimidine-purine (YR) step is more susceptible to bending deformation than a purine-pyrimidine (RY) step because it has a smaller amount of base-pair overlap.[9,10,12] (See Figures 6.4-6.6 of Dickerson[13]). But, although a YR step is inherently more bendable, it is not necessarily bent; its conformation depends on its local environment.[14] Hence,

E-mail address of the corresponding author: red@mbi.ucla.edu

0022-2836/01/051037–13 $35.00/0

the central T_3A_3 of our helix is expected to be intrinsically bendable. The largest component of bending in *B*-DNA has been shown to occur by rolling adjacent base-pairs over one another along their long axes, usually in a direction that compresses the wide major groove (positive roll).[9,14] Tilt has little effect on bending because of the high energetic costs needed to lift apart stacked bases at one end.[15]

YR steps are the most deformable of all dinucleotide pairs[16] and can adopt large roll, twist and slide values. The large roll deformations that can occur at T-A steps can facilitate bending of the helix axis, and hence these steps are usually chosen as natural fracture points by DNA-bending proteins such as catabolite activator protein and Trp repressor.[9–10] YR steps are the most deformable steps in DNA/protein complexes in general, allowing the DNA to wrap around the surface of the protein.[16] These bending properties of native A-tracts may explain why proteins usually choose pyrimidine-purine steps as the locus of bending, and involve A-tracts near that locus.[9,10,14,17,18] Moreover, studying the sequence-structure relationship of dinucleotide steps within A-tracts can reveal how sequence influences the deformability of DNA, and can lead to an understanding of DNA interactions with proteins and drugs, and in nucleosomes.

To these ends, we report the structure of the newly solved DNA decamer CCTTTAAAGG, and examine bending at T-A and A-T within A-tracts of CCTTTAAAGG and 25 previously solved native DNA structures, all of which contain at least four A or T bases at the center[2,4,6,12,19–36] (Table 1). A database approach gives an indication of the conformational flexibility of each base step and the effects of sequence *versus* crystal packing on bending parameters. A given structure provides a snapshot of one possible conformation compatible with the sequence-specific stacking requirements, the geometric constraints of the DNA, and the crystal packing.[37] The same sequence can contort in different ways, and crystal packing can influence which of these conformations it will adopt in a particular case. Thus, analyzing the structures in multiple crystallization environments makes it possible to determine the relative influences of base sequence and crystallization effects[38] when studying DNA bending.

The use of local rather than global parameters emphasizes sequence-specific base-stacking inter-

Table 1. Representative structures relevant to A-tract bending

NDB code	Sequence	Space group	Cell dimen.	Salt	Res (Å)	Reference
A. *TA sequences*						
Bd0051	**CCTTTAAAGG**	***P*2$_1$2$_1$2$_1$**	**36 39 33**	**Mg**	**1.6**	**This work**
Bdj031	CGATTAATCG	*P*2$_1$2$_1$2$_1$	39 39 33	Mg	1.5	Quintana *et al.*[12]
Bdj055	CCATTAATGG	*P*3$_2$21	33 33 96	Mg	2.3	Goodsell *et al.*[19]
Bdl059	CGCGTTAACGCG	*P*2$_1$2$_1$2$_1$	26 41 67	Mg	2.3	Balendiran *et al.*[20]
B. *AT sequences*						
Bdl038	CGCAAATTTGCG	*P*2$_1$2$_1$2$_1$	25 41 66	Mg	2.2	Edwards *et al.*[4]
Bdj069	CGCAATTGCG	*C*2	64 25 38	Mg	2.3	Wood *et al.*[21]
Udj031		*I*2$_1$2$_1$2$_1$	27 39 54	Mg	2.5	Spink *et al.*[22]
Bd0014	CGCGAATTCGCG	*R*3	41 41 100	Ca	1.4	Liu *et al.*[23]
Bd0032		*P*3$_2$12	26 26 99	K, Ba	1.8	Johansson *et al.*[24]
Bd0041		*P*2$_1$2$_1$2$_1$	26 41 67	Mg	1.2	Sines *et al.*[25]
Bdl001		*P*2$_1$2$_1$2$_1$	25 40 66	Mg	1.9	Drew *et al.*[26]
Bd0006	GGCCAATTGG	*P*2$_1$2$_1$2$_1$	26 36 53	Mg	1.2	Vlieghe *et al.*[27]
Bd0016	GCGAATTCG	*P*2$_1$2$_1$2$_1$	22 37 53	Mg	0.9	Soler-Lopez *et al.*[28]
Bd0018	GCGAATTCGCG	*H*3	39 39 99	Ca	1.3	Minasov *et al.*[29]
Bd0019	GGCGAATTCGCG	*R*3	42 42 100	Ca	1.7	Minasov *et al.*[29]
Bdl029	CGTGAATTCACG	*P*2$_1$2$_1$2$_1$	25 41 66	Mg	2.5	Larsen *et al.*[30]
C. *Pure A-tracts*						
Bdl006	CGCAAAAAAGCG	*P*2$_1$2$_1$2$_1$	25 41 66	Mg	2.5	Nelson *et al.*[2]
Bdl015	CGCAAAAATGCG	*P*2$_1$2$_1$2$_1$	25 40 66	Mg	2.6	DiGabriele *et al.*[6]
Bdl021	CGCGAAAACGCG	*P*2$_1$2$_1$2$_1$	26 44 67	Mg	3.0	Aymani *et al.*[31]
Bdl047	CGCGAAAAAACG	*P*2$_1$2$_1$2	45 66 43	Mg	2.3	DiGabriele & Steitz[32]
D. Alternating at sequences						
Bdj036	CGATATATCG	*P*2$_1$2$_1$2$_1$	39 40 34	Ca	1.7	Yuan *et al.*[33]
Bdj037		*P*2$_1$2$_1$2$_1$	39 40 34	Mg	2.0	Yuan *et al.*[33]
Bdl007	CGCATATATGCG	*P*2$_1$2$_1$2$_1$	24 39 67	Mg	2.2	Yoon *et al.*[34]
Bdl078	CGCGATATCGCG	*P*2$_1$2$_1$2$_1$	24 39 66	Mg	2.2	Shatzky-Schwartz *et al.*[35]
E. *Structure isomorphous with* T_3A_3						
Bdj025	CGATCGATCG	*P*2$_1$2$_1$2$_1$	39 40 33	Mg	1.5	Grzeskowiak *et al.*[36]

This Table lists 25 crystal structures with two different cations in 13 crystal packing environments. Where several examples are available of the same base sequence with the same cations in the same space group, only the structure of highest resolution is selected here. The decamer solved in this study is in bold face in the first row of the Table.

actions rather than external crystal packing forces.[7,38] Bending behavior observed in these 25 structures is relevant to protein/DNA complexes because, as has been noted before,[9] the local DNA environment in the crystal is a better model for a DNA/protein complex than is an isolated DNA molecule in solution. The fact that bending trends observed in crystalline protein/DNA complexes are determined largely by the bound protein rather than by crystal packing,[37] gives credence to the idea that one can get past crystal packing to discover innate sequence-structure relationships. Because flanking sequences have a large influence on base step geometry,[39] it is important to understand whether a T-A step behaves similarly when it lies within A-tracts *versus* random sequences. That is, how do A-tracts influence T-A and A-T steps?

Here, the terms T-A, A-T, pure A-tract and alternating A-T tract will refer to decamer or dodecamers whose central four base-pairs are TTAA, AATT, AAAA and ATAT, respectively. Unless stated otherwise, only free DNA is considered, not DNA complexes with proteins, drugs, or other molecules.

Results

Crystal packing

Packing forces undeniably influence how a structure bends. Like most decamers with one helical turn per molecule, each CCTTTAAAGG helix (designated T_3A_3) is stacked end-on-end as a pseudo-continuous helix with an average of 9.44 residues per helical turn (Figure 1(a)). The step between two stacked helices can be considered a normal base step despite the lack of phosphate backbone connecting the two base-pairs. The main contacts of a given helix with its neighbors are between terminal base-pairs within one stack (Figure 1(b)). Because the helices pack parallel with one another, some lateral inter-helical contacts occur along the sugar/phosphate backbone, whereas the only base-base contacts occur between bases T4 and A16. (Strand 1 contains bases C1 through G10, and strand 2 contains C11 through G20, both in a 5′-to-3′ direction.) This packing is seen also in CGATTAATCG[12] and CGATATATCG,[33] which are isomorphous with T_3A_3. Three interstrand bifurcated hydrogen bonds form across the minor groove. They occur between O-2 of T3 and N-2 of G19, between N-2 of G9 and O-2 of T13, and between N-2 of G10 and O-2 of C12.

Bending and helical parameters

Base-pair normal vectors are a convenient graphic means of displaying bending behavior. As diagrammed in Figure 3 of Dickerson,[14] the normal vector lies perpendicular to the best mean plane through all atoms of a base-pair. As the helix bends, this normal vector changes orientation. It is a useful gauge of helix bending because the base-pairs in *B*-DNA are effectively perpendicular to the helix axis. The angle between successive base-pair normal vectors, or VALL,[13] reveals that a bend of 8.6° occurs at base step T5-A6, while those of the surrounding steps cluster around 2.0° (Figure 2(a)). This 8.6° bend is entirely ascribable to roll (Figure 2(b)); the tilt component is negligible. Roll also is the primary mode of DNA bending in other crystal structures, and is especially important for bending of DNA around proteins.[9,15,37] A plot of base-pair normal vectors (Figure 2(c)) shows the 8.56° bend at the central T-A step. The helix is separated into two segments with a large change in direction at the T-A step. The first segment, consisting of C1 through T5, writhes gently toward the upper left-hand corner of the plot as depicted by the first red arrow. After a large change in direction at the central T5-A6 step (second red arrow), the final segment consisting of A6 through G10 writhes gently towards the bottom of the plot (third red arrow). A large positive roll widens the minor groove as it compresses the major groove. The minor groove is narrow near the ends of the duplex and widens gradually to 7.9 Å at the T5:A16 base-pair.

Geometric restrictions of the sugar/phosphate backbone and steric restraints cause rise, slide, cup, and twist to change along with roll.[39,40] Yanagi *et al*.[39] considered this correlation and found it useful to define a quantity called the profile sum:

$$\text{Profile sum} = (\omega - 36) - 16.24(D_z - 3.36) + 0.744\chi - 0.703\rho$$

where ω is twist, D_z is rise along the helix axis, χ is cup and ρ is roll. The profile sum correlations, as Yanagi *et al*. observed, arise mainly from finite constraints of backbone chain length between bases. The stretching of backbone chain that arises from large twist at high twist profile (HTP) steps is relieved by keeping the base-pairs close to one another (D_z), bringing the ends closer *via* positive cup (χ), and avoiding excessive roll (ρ). Conversely, a small twist angle provides slack in the backbone chain that permits the other variables more freedom. The central T-A step of T_3A_3 has a low twist profile (LTP; profile sum $\leqslant -10$), with positive roll, low twist, high rise, and negative cup (Table 2, line 1). Base pairs surrounding the T-A step, however, have an HTP (profile sum $\geqslant 10$), with negative roll, high twist, low rise, and positive cup. This same profile behavior for the central and surrounding steps has been observed in CGATTAATCG and CGATATATCG, which also have a widened minor groove at the central four base steps. T-A steps, in general, display variable profile sums,[12] so it is not surprising that this central T-A step disrupting the A-tract is underwound compared with neighboring steps when, on average, a T-A step in general is overwound.[40]

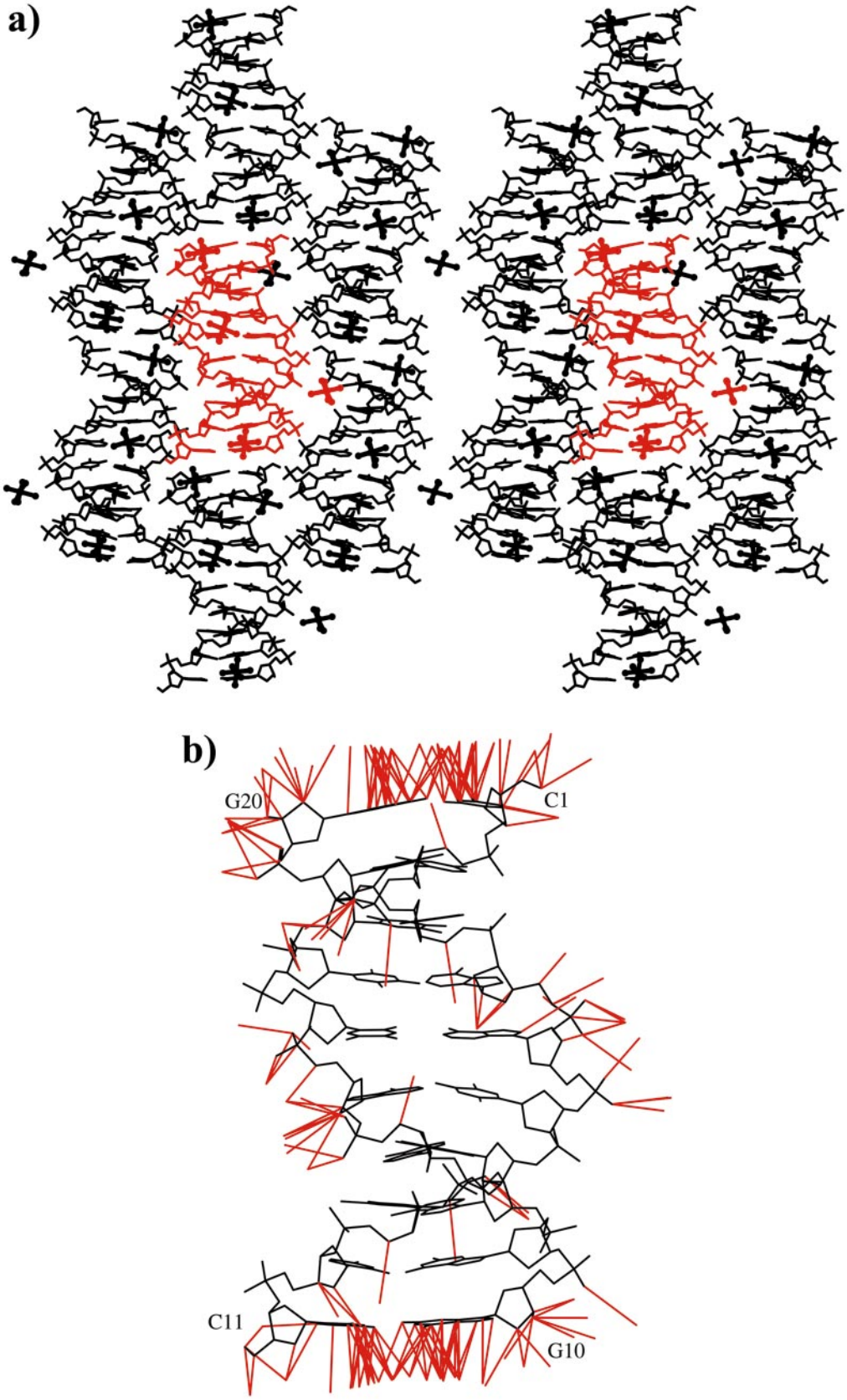

Figure 1. Crystal packing of T_3A_3 and inter-helical contacts. (a) A MOLSCRIPT[56] stereo plot demonstrates that the DNA decamers are stacked end-on-end along the *a* axis to form pseudo-continuous helices, which are packed against each other along the *b* and *c* axes. The six neighboring helices surrounding the main red helix show the 2_1 screw axis along the *a* direction. The major groove of the central helix opens towards the viewer at the center. Notice that the step between helices is almost indistinguishable from internal helix steps. Water molecules are omitted for clarity. (b) Inter-helical contacts of 3.8 Å or less between the central helix and neighboring symmetry-related helices are shown as red lines in this MOLSCRIPT plot. The major groove again faces outward at the middle of the helix.

Table 2. Helical parameters of the central base step

NDB code	Sequence	Central base step					
		Roll	VALL	Slide	Twist	Rise	Cup
A. *TA sequences*							
Bd0051	**CCTTTAAAGG**	**8.57**	**8.56**	**0.77**	**27.73**	**3.92**	**−14.39**
Bdj031	CGATTAATCG	9.11	9.12	0.53	31.10	3.97	−10.59
Bdj055	CCATTAATGG	8.51	8.57	−0.04	38.42	3.10	12.98
Bdl059	CGCGTTAACGCG	5.66	6.57	0.17	42.30	2.90	16.60
	Average	7.96	8.21	0.36	34.89	3.47	1.15
	Standard deviation	1.56	1.12	0.36	6.66	0.55	15.90
B. *AT sequences*							
Bdl038	CGCAAATTTGCG	−2.83	2.93	−0.63	29.52	3.31	3.39
Bdj069	CGCAATTGCG	−3.91	4.00	−0.52	30.99	3.37	−4.84
Udj031		−9.74	9.70	−0.05	36.75	2.90	−4.58
Bd0014	CGCGAATTCGCG	−8.24	8.23	−0.48	35.95	3.09	−1.43
Bd0032		−5.65	5.64	−0.81	35.05	2.55	−0.21
Bd0041		−4.87	4.87	−0.57	33.32	3.18	1.56
Bdl001		−6.06	6.26	−0.06	31.82	3.12	1.12
Bd0006[a]	GGCCAATTGG	−6.02	6.10	−0.41	31.16	3.27	−1.02
Bd0016[a]	GCGAATTCG	−3.12	3.17	−0.53	30.89	3.13	4.25
Bd0018	GCGAATTCGCG	−6.77	6.76	−0.53	34.05	3.02	2.71
Bd0019	GGCGAATTCGCG	−5.68	5.75	−0.53	34.99	3.04	−2.70
Bdl029		−4.98	5.13	−0.49	32.82	3.10	1.62
	Average	−5.66	5.71	−0.47	33.11	3.09	−0.01
	Standard deviation	1.99	1.95	0.22	2.28	0.21	2.99
C. *Pure A-tracts*							
Bdl006[a]	CGCAAAAAAGCG	1.45	1.64	−0.74	38.67	3.02	12.89
Bdl015[a]	CGCAAAAATGCG	3.03	3.18	−0.52	36.35	3.28	−0.03
Bdl021	CGCGAAAACGCG	−1.82	7.12	−2.22	34.27	3.22	2.36
Bdl047[a]	CGCGAAAAAACG	0.92	1.30	−0.54	34.93	2.92	−3.96
	Average	0.90	3.31	−1.01	36.06	3.11	2.82
	Standard deviation	2.02	2.67	0.82	1.95	0.17	7.20
D. *Alternating at sequences*							
Bdj036	CGATATATCG	5.27	5.35	0.04	25.05	3.88	−5.99
Bdj037		6.42	6.42	−0.09	24.55	3.87	−7.02
Bdl007	CGCATATATGCG	−0.34	0.56	−0.57	28.76	3.64	−11.53
Bdl078	CGCGATATCGCG	6.52	6.64	−0.87	34.86	3.16	11.62
	Average	4.47	4.74	−0.37	28.31	3.64	−3.23
	Standard deviation	3.25	2.84	0.42	4.76	0.34	10.19
E. *Structure isomorphous with* T_3A_3							
Bdj025	CGATCGATCTG	8.47	8.46	0.60	29.25	4.07	−4.42

[a] These sequences had multiple structures, but only the parameters for the first structure are listed here.

Hydration of the minor groove and cations

In T_3A_3, a zigzag spine of hydration similar to that first observed in the Drew dodecamer[26] is interrupted at the central base step (Figure 3). Water molecules of the first shell (larger red spheres) hydrogen bond to O-2 of pyrimidines and N-3 of purines. Water molecules of the second shell (smaller red spheres) hydrogen bond to the first-shell water molecules, creating the zigzag pattern. Magnesium ion complexes Mg1 and Mg3 disrupt this spine of hydration at either end of the decamer, so that two water molecules of the first hydration layer become coordinated to the magnesium ion, which replaces the water molecule of the second hydration shell.

The central magnesium ion (Mg2) sits within a widened minor groove, with two of its coordinated water molecules interacting with T5 O-2 and A17 N-3, just as had been found with the isomorphous CGATTAATCG.[12] As with that structure, this same magnesium complex bridges across to two backbone phosphate groups of a neighboring helix, and hence the specific location of the complex along the minor groove probably is to be ascribed to crystal packing. The last magnesium ion (Mg4) lies in the major groove and contacts G19 O-6 as well as A18 N-6 and A18 N-7.

Even without any disruption by magnesium complexes, water molecules no longer form a zigzag spine when the minor groove widens. The water molecules contacting the T-A step (Wat1 and Wat2), reside side-by-side instead of vertically, to allow the spine of hydration to bridge the widest part of the minor groove. This double bridge or double row of water molecules seen only at the T-A step in T_3A_3 was encountered along the entire wide minor groove region of CCAACGTTGG.[41] Disruption of the spine of hydration at the T-A step is expected from theoretical calculations.[42] Doubling of the spine within this region allows each water molecule to contact only one strand,

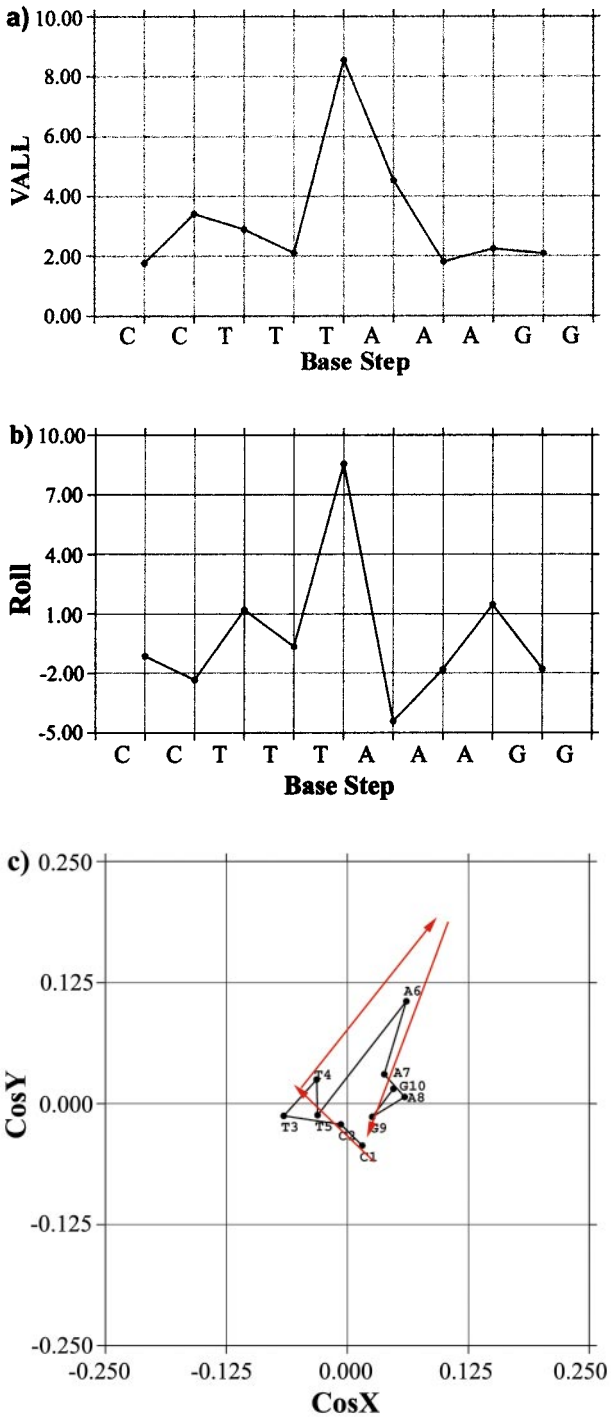

Figure 2. Bending of T_3A_3: VALL, roll, and base-pair normals. (a) Plot of the angle between successive base-pairs (VALL) demonstrates the large bend at the T-A step of T_3A_3. (b) This bend at the central T-A step is mostly because of positive roll, which compresses the minor groove. (c) The bend also is evident in a plot of base-pair normals. In such a plot, all the vectors perpendicular to individual base-pairs are brought to a common origin and viewed along the overall helix axis. Each labeled point in the plot marks the tip of one vector. Bending is evidenced by migration of these points across the diagram. Red arrows indicate the direction of overall bend for each segment of the helix. (For further explanatory diagrams of normal vectors, see Figures 3, 8 and 14 of Dickerson,[14] or Figure 4 of Dickerson & Chiu.[10])

whereas in A-tracts or any other narrow minor groove region the spine interacts with both strands.[42]

Sugar pucker

The central magnesium ion (Mg2) may also influence sugar pucker. All of the sugars except that of A17 fall within the normal *B*-DNA continuum centered on the C2′-*endo* sugar conformation. The sugar moiety of A17, however, has a C3′-*endo* conformation usually observed only in RNA. Its pseudorotation dihedral angle is 13.4° compared to 103°-144° for the other sugars. Crystal packing forces cause this anomaly. Structures isomorphous with T_3A_3, CGATTAATCG, CGATATATCG, and CGATCGATCG, have the same conformation at base A17 regardless of sequence because of their similar crystal packing. The A17 sugar of CGATTAATCG, for example, has a pseudorotation angle of 18.9° compared to 110°-184° for the other sugars. The A17 sugar in CGATATATCG has a pseudorotation angle of 48.2° and 50.5° in the presence of Ca^{2+} and Mg^{2+}, respectively, whereas the corresponding values for its other sugars are 118°-197° and 94°-206°. Similarly, the A17 sugar of CGATCGATCG has a psuedorotation angle of 36.1°, while its other sugar moieties range from 107° to 180°. In these structures, sugar 17 has close contacts with the sugar/phosphate backbone of residue 3 from a neighboring helix, and with a cation in the minor groove. These contacts are most likely the cause of this switch from a DNA to a C3′-*endo* RNA sugar pucker, as was surmised by Quintana *et al*.[12]

Discussion

The 25 crystal representative structures containing A-tracts listed in Table 1 include 13 different crystal packing environments and two different divalent cations. Monovalent cations are not considered in this study because they have minimal influence on the structure of *B*-form DNA.[43] However, structures with different crystal packing are included in this study in order to reveal the range of possible conformations for a given dinucleotide step.

Bending *via* roll

Only the local bend is discussed below. Bending caused by a particular step in oligomers is not portrayed accurately by global bending, because a bend at a given step can be negated by other bends within the structure. In addition, the overall bend often is an artifact of crystal packing, while local structural features are more likely to be caused by sequence rather than the crystal lattice.[6] Local bending can be quantified with VALL, which represents the angle between successive base-pair normals. The average VALL values for central steps of the T-A, A-T, and A-A structures are 8.2°,

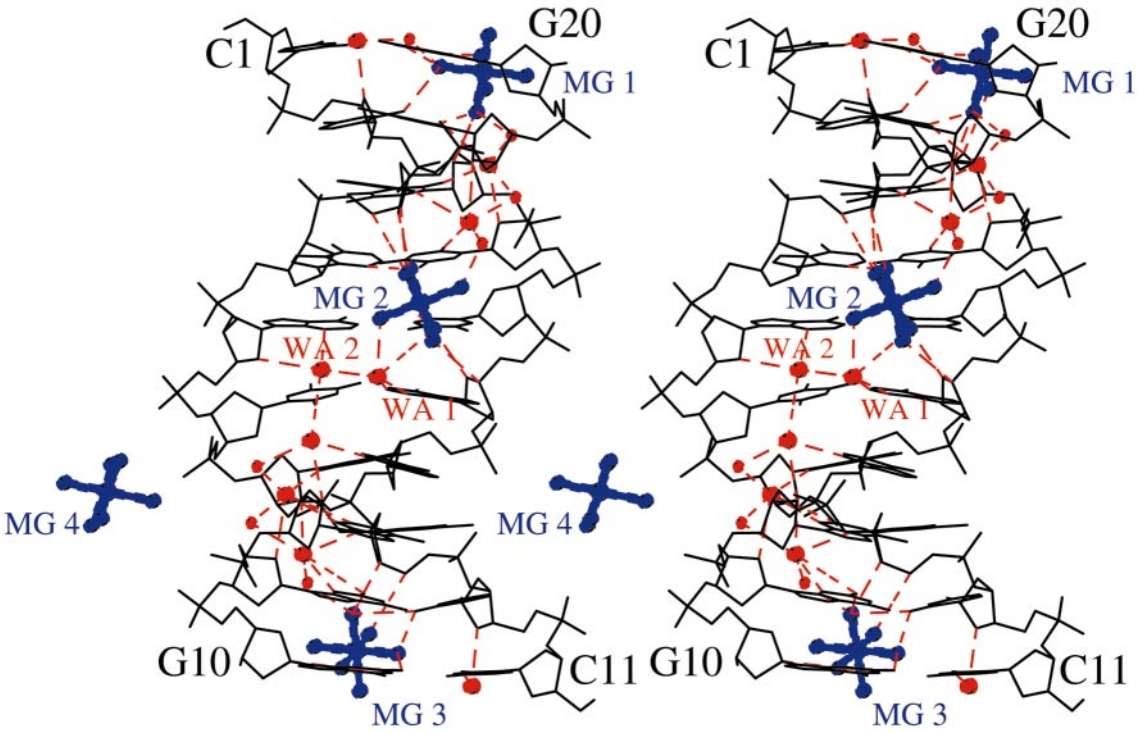

Figure 3. T_3A_3 minor groove hydration pattern. MOLSCRIPT stereo drawings depict a single zigzagged spine of hydration interrupted at the central T-A step. The minor groove is facing outward. Water molecules of the first and second hydration layer are depicted as large and small red spheres, respectively. The four octahedrally coordinated magnesium complexes of the asymmetric unit are in blue. On the back side of the molecule as drawn here, the central carbonyl oxygen atoms of T5 and T15 accept hydrogen bonds from a tetrahedrally coordinated major groove water molecule (C═O—W distances, 2.57 Å and 2.59 Å for T5 and T15, respectively), exactly as is seen in the familiar spine of hydration along the minor groove.

5.7°, and 3.3° (Table 2), respectively, indicating that a T-A step within an A-tract is inherently more bent than are A-T and A-A steps in a comparable environment, as expected. Although T-A steps tend to be more bendable, four A-T steps show a larger bend than these central T-A steps because of packing constraints. This distortion of the A-T sequences may skew the apparent difference in bending between the two kinds of steps, but the size of the database for the A-T sequences should be large enough to overcome this potential problem.

As in T_3A_3, bending is seen to occur almost exclusively *via* rolling, because the absolute value of roll is approximately the same as the VALL values, whereas tilt is negligible (Table 2). Average roll values for the central T-A, A-T and A-A steps are 8.0°, −5.7° and 0.9°, respectively, (notice the similarity to the average VALL values), indicating that roll-associated bending occurs at T-A and A-T steps but not within pure A-tracts. Although A-tract and A-T step sequences have often been considered to be equivalent, many of their local parameters are drastically different, so the remainder of this analysis will focus mainly on A-T and T-A step sequences. The tendency of RY steps to have a small negative roll and Y-R to have a large positive roll was observed previously[26,44] and was predicted by theoretical free energy calculations.[45] No exceptions to this trend occur, even though structures have different packing, cations, and sequence (Table 1), showing how strongly T-A and A-T steps in an A-tract favor positive and negative roll values, respectively.

Although the difference in intrinsic bending is slight, T-A and A-T steps bend the DNA in a different manner. T-A steps bends DNA toward the major groove, while A-T steps bend DNA toward the minor groove. The same behavior is observed in DNA bound to proteins and drugs.[8] For example, catabolite activator protein bends DNA toward the major groove at T-A steps but in the opposite direction at A-T and A-A/T-T steps.[46] Bending towards the minor groove is more costly because of the narrow groove width and physical constraints of the sugar/phosphate backbone. This considerable energetic difference between bending towards the major *versus* minor groove may be the reason why proteins prefer T-A steps to A-T steps in bending DNA.

Deformability of T-A *versus* A-T steps and their helical parameters

It has been hypothesized that T-A steps are much more deformable than most dinucleotide steps because of the lack of base stacking interactions. These stacking inteactions have been noted many times, and are particularly well illustrated in Figures 6.4-6.6 of Kravilis.[56] Analysis of the base steps within 60 naked DNA oligomers[44] showed that T-A steps, with their large spread of helical twist, roll, and slide, are loose or continuously flexible, while AA/TT and A-T steps are the most rigid of all the dinucleotide base steps, with helical parameters that cluster around one conformation. Bases are considered deformable when they have a large conformational range of helical parameters.[37]

In this study, the difference in deformability between T-A and A-T steps within A-tracts is most striking with cup, which has the largest difference in standard deviation from 15.90° for T-A steps to 2.99° for A-T steps (Table 2). The T-A structures always have a larger magnitude of cup at the central step between 10.5° and 17°, compared to 0° and 8° for A-T steps, even though some of the A-T structures show a larger magnitude of roll. By definition, cup is the change in buckle between two successive base-pairs, and hence buckle also demonstrates a large deformability of T-A steps. The deformability of cup in T-A steps most probably derives precisely from the smaller stacking overlap of base-pairs. Stacking overlap would tend to keep the base-pairs flat.

The deformability of T-A steps can be seen with minor groove width, which is most variable at T-A steps (Figure 4). The minor groove width of T_3A_3 in CCTTTAAAGGG isomorphous structures varies smoothly and is widest at the central step (Figure 4(b)). However, two other T-A sequences, which have different crystal packing environments (Figure 4(a)) show a narrowing of the minor groove instead. At first, the narrow minor groove seems contradictory to the large positive roll deformation that compresses the major groove of these sequences and thus should widen the minor groove. But the internal mechanics of *B*-DNA allow the minor groove to narrow by other means besides bending (e.g. roll).[47]

The narrow minor groove width of CGCGTTAACGCG is similar to those of the isomorphous CGCGAATTCGCG, CGCATATATGCG, and CGCGATATCGCG (Table 1 and Figure 4(c)), regardless of the sequence at the central step. Thus, minor groove widths of T-A sequences are variable, but more similar among crystal isomorphs. This demonstrates that crystal packing has a large influence in determining minor groove width for such a deformable step as T-A.

T-A steps also show an intrinsic deformability or variety of helix parameter values with the variable twist; both high and low twist values are encountered. The central T-A steps adopt twist values both higher and lower than central A-T steps,

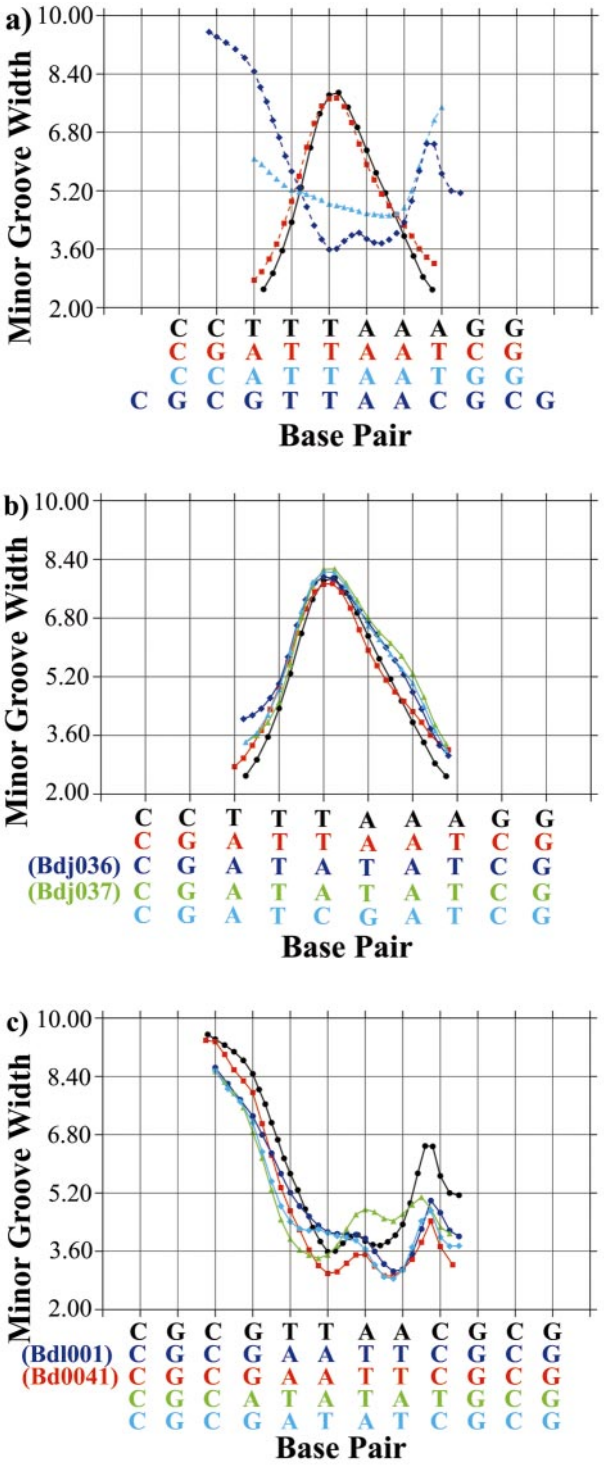

Figure 4. Minor groove width of T-A sequences and their isomorphous structures. The minor groove width was calculated by CURVES.[55] (a) The four TA structures vary in minor groove width depending on crystal packing. (b) CCTTTAAAGG, CGATTAATCG, and their isomorphous $P2_12_12_1$ decamers have a widened minor groove at the center. But CGATCGATCG, which has no A-tract, shows that packing can lead to a widened minor groove even without an A-tract. (c) The minor groove of CGCGTTAACGCG and its isomorphous $P2_12_12_1$ dodecamers have very similar minor groove widths.

which center around one twist conformation (Table 2). T-A steps have a larger standard deviation of twist, 6.66°, compared to 2.28° for the A-T sequences (Table 2). On average, T-A steps have a higher twist of 34.89° compared to 33.11° for A-T steps. This trend is consistent with other *B*-DNA structures[40] and protein/DNA complexes.[16]

At the central step, sequences isomorphous with T_3A_3 including CGATTAATCG have a low twist profile and a wide minor groove, while other T-A sequences, A-T sequences, and pure A-tracts have an intermediate or high twist profile and a narrow minor groove (Table 2). Because the minor groove widens when the T-A step is underwound, minor groove and twist are correlated.

Deformability of the T-A step is also seen with rise, which for the T-A steps has a standard deviation of 0.55 Å compared to 0.21 Å for A-T steps (Table 2). Although rise does not vary as much as other helical parameters, the difference could be significant because dinucleotide steps in the naked DNA database[44] have a rise of 3.4 Å over 70% of the time. For T_3A_3, CGATTAATCG and their isomorphous structures, the rise peaks to ~4 Å at the central step from ~3 Å (Figure 5(a)). This large increase in rise may accommodate the bending of the central step, allowing the bases to avoid steric clashes that would be caused by the large positive roll of the step. This large increase in rise is not seen with the other two T-A sequences (Figure 5(b)), so perhaps overwinding relieves the energetic cost of bending in these sequences by twisting the ends of the cupped bases away from one another. These T-A sequences have different rise values, even though they all bend between 6.5° and 9°.

Because rise is measured with the sugar C-1′ atoms located at the base-pair extremities, rise values are affected by large cup deformations. A large negative cup, like that in T_3A_3 and CGATTAATCG, will give a deceptively large rise, whereas a large positive cup as seen with CCATTAATGG and CGCGTTAACGCG will give a deceptively small rise.[39,44] A-T steps do not have large cup values, so their rise values are not as deceptive.

Even though all the central T-A steps have a high roll and a high roll usually corresponds to a low slide,[37,44] this analysis shows that T-A steps can adopt low or high values of slide depending on crystal packing. The central steps of T_3A_3 and CGATTAATCG, which have a widened minor groove and low helical twist, also have a larger slide than any of the A-T sequences (Table 2). The magnitude of slide of the other two T-A sequences is closer to the A-T sequences. All central T-A steps show an increase in slide from the previous step, while the central A-T steps decrease (Table 2). Because the average slide is 0.36° for T-A steps and −0.47° for A-T steps, they are sliding in different directions, probably to accommodate positive and negative roll. The standard deviations of slide for T-A steps and A-T steps are 0.36 Å and 0.22 Å,

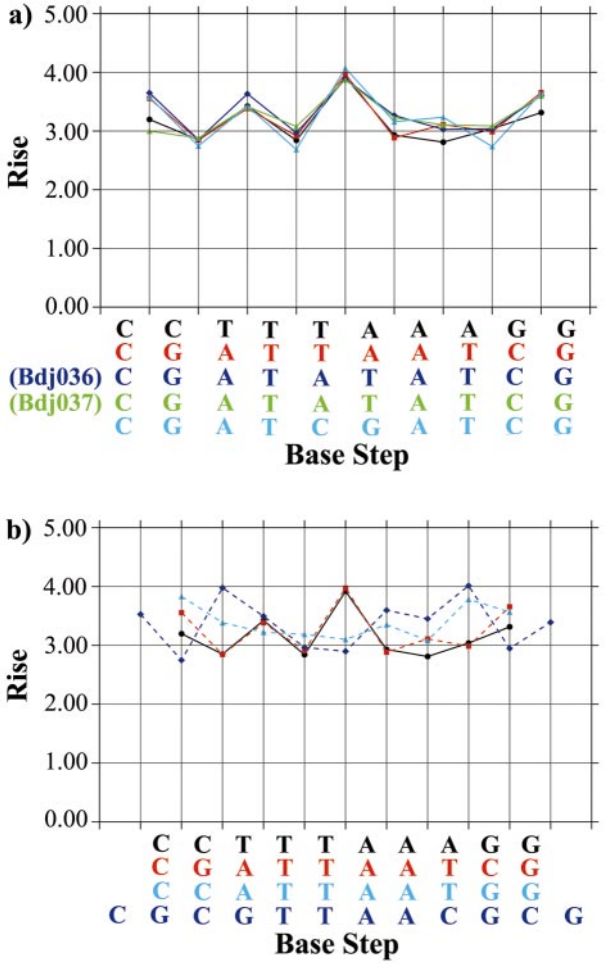

Figure 5. Deformability of TA sequences as demonstrated by rise. (a) T_3A_3 and its four isomorphous sequences show an increase in rise of ca 1.0 Å at the central step. (b) The four TA sequences show a variety of rise values at the central step, although they all bend by 6.5° to 9°. Again, the rise values of the TA sequences are more similar to their isomorphous sequences than to each other. This demonstrates the flexibility of the T-A step.

closer than expected because of the small sample size of the T-A sequences. When more T-A steps were analyzed, a larger continuous range of slide was seen and, in fact, slide was one of three parameters used to determine the deformability of dinucleotide steps.[44,48] The neighboring sequence affects slide more than any other parameter because of constraints of the DNA backbone.[49] Thus, the smaller range in slide may occur because all the T-A steps lie within an A-tract and thus have less variation than T-A steps within random sequences with different neighbors.

The rigidity of the A-T and AA/TT steps may be a result of the large propeller twisting at these steps. The A-T steps, like pure A-tracts, are highly propeller-twisted with average values of −16.75° and −17.19° for the two base-pairs of the central

A-T steps, while the T-A steps are not as propeller-twisted with average values of −15.71° and −14.25° (Table 2). R-R/Y-Y and R-Y steps have a higher propensity for propeller twisting than Y-R steps because they have no steric penalty to propeller twisting, and this sequence-specific tendency hinders the conformational stability of the dinucleotide steps, making the A-A/Y-Y and A-T steps more rigid.[37] For instance, the less propeller twisted bases are freer to slide past one another. Thus, the highly propeller twisted A-T and A-A steps have a negative slide averaging −0.49, whereas the less propeller twisted T-A steps have an average slide of 0.36. This negative correlation between slide and propeller twist was seen also with T-A steps in random sequences.[37]

Comparing the four structures containing a TTAA as the central base-pairs in three different crystal packing environments has shown that T-A steps cause the DNA to adopt different conformations, which all demonstrate a positive roll but have different behaviors in minor groove width, slide, twist, and rise. T_3A_3 and CGATTAATCG (as well as CGATATATCG), have a wide minor groove, large slide, low twist, and a large rise, indicating a correlation among these parameters. The other two, however, have a narrow minor groove, a small slide, a high twist, and a low rise.

Alternating A-T sequences have variable conformations

The central A-T steps of the alternating A-T sequences CGATATATCG, CGCATATATGCG, and CGCGATATCGCG have conformations that logically resemble an A-T step, a T-A step, or in-between. For example, at the central step, they bend approximately the same amount as the A-T sequences but bend with a positive roll like the T-A sequences. This different behavior of the A-T steps within an alternating A-T context as opposed to within an A-tract demonstrates the importance of neighboring base steps. T-A steps are extremely variable even in the same sequence context, while A-T steps appear to center around one conformation in the same context but vary between contexts. Proteins can recognize the contextual difference as well. The preference for alternating A-T/T-A steps at the beginning of the TATA box, and for pure A-A steps at the end, have been proposed to be important for determining binding directionality of the universal transcription factor TATA-binding-protein.[50]

Concluding remarks

By analyzing T-A steps only within A-tracts, this study demonstrates that T-A steps are inherently deformable, bendable, and variable, even within the same sequence context. This variability is seen despite the small sample size of T-A sequences. This deformability is so inherent to T-A sequences that the four T-A structures in three crystal packing environments show more variation than the 23 A-T structures in eight different environments. Even larger ranges of helical parameters should be seen when more crystal structures are solved.

In summary, the larger deformability of a T-A step, compared to A-T and A-A steps, can be seen by the large range of twist, rise, cup, and buckle as well as different trends in minor groove width. The standard deviations of twist, rise, and cup are 6.66°, 0.55 Å, and 15.90° for T-A steps compared to 2.28°, 0.21 Å, and 2.99° for A-T steps, which are more rigid. Although these parameters do not cause bending within A-tracts, together they contribute to the large roll angle of the T-A step. Remember that the steric hindrances of the bases and geometric constraints of the DNA backbone[40] cause certain helical parameters to be correlated. Despite the large variability of the other parameters, T-A steps within A-tracts have a large positive roll. The standard deviation of roll for T-A steps, 1.56°, is actually smaller than the standard deviation of A-T steps, 1.99°. Thus T-A steps within A-tracts bend toward the major groove and are highly deformable and variable, allowing them (but not necessarily requiring them) to be natural fracture points of the helix. A-T steps, in contrast, bend slightly toward the minor groove and are more rigid.

Materials and Methods

The structure of the decamer CCTTTAAAGG was solved by molecular replacement using CNS,[53] by rigidly refining the position of a related decamer in an isomorphous cell.

Oligonucleotide synthesis, crystallization, and data collection

The decamer was synthesized on an Eppendorf ECOSYN D300 synthesizer at a 5 μmol scale. Base-protecting groups were removed by deprotecting with NH_4OH at 55 °C for 16 hours. The DNA then was loaded onto a 50 g Dupont Nensorb reverse phase column that had been pre-washed with 100% MeOH and 0.1 M triethylamine acetate (TEAA). This column was washed with 0.1 M TEAA, followed by 12% (v/v) acetonitrile to remove failure sequences. At this point, only full-length DNA remained on the column because it is the only species that still has a trityl group. To remove the trityl group from the DNA, the column was washed with 0.5% (v/v) trifluoroacetic acid (TFA), and the cleaved trityl group and TFA were removed by washing with 0.1 M TEAA. The column then was washed with double-distilled water (ddH_2O) to remove the TEAA. Finally, the DNA was eluted from the column with 35% (v/v) MeOH. The MeOH then was removed by rotovaping, followed by lyophilization until the sample was dry. The sample was stored at −80 °C in ddH_2O.

Crystals were obtained by sitting-drop vapor diffusion at 4 °C in a nine-well plate. A crystallization droplet containing 0.6 ml of 0.86 mM CCTTTAAAGG double helix, 0.35 mM spermine hydrochloride, 5.00 mM magnesium acetate, and 12.5% (v/v) 2-methyl-2,4-pentanediol (MPD) was equilibrated against a reservoir of 20%

MPD. The MPD in the reservoir solution was incremented by 5 % every two weeks up to 30 %, at which point crystals appeared. Diffraction data were collected on a Rigaku RAXIS-IV image plate detector and processed with the HKL package.[51] Data collection statistics are listed in Table 3.

Structure determination

The structure was solved by molecular replacement using CGATATATCG (NDB bdj036) as a starting model and incorporating the proper base substitutions in O.[52] Approximately 10 % of the reflections were set aside randomly for structure validation with the free-*R* test. Initial rigid-body refinement, incrementing from the whole duplex, a single strand, two bodies per strand, and individual residues, was carried out to 3 Å in CNS.[53] Slow-cool-simulated anneal, group temperature factor refinement, and individual temperature factor refinement were then performed to 2.5 Å. Refinement continued with two more rounds of slowcool-simulated anneal and individual temperature factor refinement adding all the data to 1.6 Å. The first water molecules and three magnesium ions were modeled into the electron density between those two rounds. High-resolution refinement was continued in Shelxl-97.[54] After optimizing the SWAT, HOPE, and EXTI parameters, one magnesium ion and more water molecules were added to the model. Magnesium complexes were restrained to be in octahedral geometry, with bond length ca 2.1 Å. Solvent atoms were added iteratively to the difference map above 3.0 σ and finally, WGHT, DEFS, ISOR, and SIMU

Table 3. Data collection, refinement and final model statistics

A. *Data collection*

Space group	$P2_12_12_1$
Unit cell dimensions (Å)	35.558, 38.737, 32.508
Resolution range (Å)	40.0-1.6
Number of observed reflections	65,685 (6263 unique)
Redundancy	10.5

Resolution minimum (Å)	Resolution maximum (Å)	I/σ	Data completeness (%)	R_{sym} (%)
40.0	2.74	36.71	99.0	6.3
2.74	2.17	25.03	100.0	8.4
2.17	1.90	18.79	99.8	12.9
1.90	1.72	16.25	99.2	18.3
1.72	1.60	11.17	98.0	26.8
All Reflections		26.22	99.2	8.4

B. *Structure refinement*

Cycle	Program	Processes completed during stage	Resolution (Å)	R_{cryst} (%)	R_{free} (%)
1	CNS	Rigid body	40-3.0	37.05	48.86
2		Simulated anneal, group & individual *B*-factor	40-2.5	31.95	38.57
3		Simulated anneal, individual *B*-factor	40-1.6	27.87	33.28
4	Shelxl	SWAT, HOPE, EXTI	40-1.6	25.11	31.56
5		FLAT, solvent addition	40-1.6	18.75	26.55
6		Optimize WGHT, DEFS, ISOR, SIMU	40-1.6	17.51	23.93
7		**Final model**	40-1.6	17.94	23.64

C. *Final model statistics*

Resolution minimum (Å)	Resolution maximum (Å)	R_{cryst} (%)	R_{free} (%)
40.0	2.74	21.47	27.19
2.74	2.17	20.95	26.15
2.17	1.90	20.92	20.71
1.90	1.72	21.00	26.76
1.72	1.60	25.18	32.28
40.0	1.60	17.94	23.64

RMSD bonds (Å)	0.013
RMSD angles (deg.)	2.32

	Avg. *B*-factor (Å^2)	No. atoms
DNA	9.3±2.8	404
Solvent	18.9±7.9	137
Overall	11.8±6.2	541

$R_{sym} = \Sigma_{hkl}\Sigma_i|I_i - \langle I\rangle|/\Sigma_{hkl}\Sigma_i I_i$, where I_i is the intensity of each symmetry-related reflection and $\langle I\rangle$ is their average.
$R_{cryst,\ free} = \Sigma_{hkl}|F_{obs} - F_{calc}|/\Sigma_{hkl}F_{obs}$.

parameters were optimized. Each session of refinement was preceded by model building in O. With each stage of refinement, R_{cryst} and R_{free} decreased until they leveled off at around 18 % and 24 %, respectively. The difference between R_{cryst} and R_{free} began at 11.8 % and decreased to 5.7 %. Refinement statistics are given in Table 3. DNA helical parameters were calculated with CURVES[55] and FREEHELIX97,[14] and plotted with SHELXDNA.[42]

Data Bank accession numbers

The PDB and NDB accession numbers are 1IKK and Bd0051, respectively.

Acknowledgments

We thank Mary L. Kopka for her advice during the preparation of this manuscript, as well as the Dickerson group for all their help and support. Funding was provided by the National Institute of Health (NIH Program Project Grant GM-31299).

References

1. Dickerson, R. E. (1999). Helix structure and molecular recognition by *B*-DNA. In *Oxford Handbook of Nucleic Structure* (Neidle, S., ed.), p. 181, Oxford University Press Inc., New York.
2. Nelson, H. C. M., Finch, J. T., Luisi, B. F. & Klug, A. (1987). The structure of an oligo(dA).oligo(dT) tract and its biological implications. *Nature,* **330**, 221-226.
3. Coll, M., Frederick, C. A., Wang, A. H.-J. & Rich, A. (1987). A bifurcated hydrogen-bonded conformation in the d(A-T) base-pairs of the DNA dodecamer d(CGCAAATTTGCG) and its complex with distamycin. *Proc. Natl Acad. Sci. USA,* **84**, 8385-8389.
4. Edwards, K. J., Brown, D. G., Spink, N., Skelly, J. V. & Neidle, S. (1992). Molecular stucture of the *B*-DNA dodecamer d(CGCAAATTTGCG)2: an examination of propeller twist and minor-groove water structure at 2.2 Å resolution. *J. Mol. Biol.* **226**, 1161-1173.
5. Xuan, J.-C. & Weber, I. T. (1992). Crystal structure of a *B*-DNA dodecamer containing inosine, d(CGCIAATTCGCG), at 2.4 Å resolution and its comparison with other *B*-DNA dodecamers. *Nucl. Acids. Res.* **20**, 5457-5464.
6. DiGabriele, A. D., Sanderson, M. R. & Steitz, T. A. (1989). Crystal lattice packing is important in determining the bend of a DNA dodecamer containing an adenine tract. *Proc. Natl Acad. Sci. USA,* **86**, 1816-1820.
7. Grzeskowiak, K., Goodsell, D. S., Kaczor-Grzeskowiak, M., Cacsio, D. & Dickerson, R. E. (1993). Crystallographic analysis of CCAAGCTTGG and its implications for bending in *B*-DNA. *Biochemistry,* **32**, 8923-8931.
8. Young, M. A., Ravishanker, G., Beveridge, D. L. & Berman, H. (1995). Analysis of local helix bending in crystal structures of DNA oligonucleodites and DNA-protein complexes. *Biophys. J.* **68**, 2454-2468.
9. Dickerson, R. E. (1998). Sequence-dependent *B*-DNA conformation in crystals and protein complexes. In *Structure, Motion, Interaction and Expression of Biological Macromolecules: Proceedings of the Tenth Conversation, State University, New York, Albany, NY* (Sarma, R. H. & Sarma, M. H., eds), pp. 17-36, Adenine Press, Albany, NY.
10. Dickerson, R. E. & Chiu, T. K. (1997). Helix bending as a factor in protein/DNA recognition. *Biopolymers (Nucleic Acid Sci.),* **44**, 361-403.
11. Hunter, C. A. (1993). Sequence dependent DNA structure; the role of base stacking interactions. *J. Mol. Biol.* **230**, 1025-1054.
12. Quintana, J. R., Grzeskowiak, K. Y. & Dickerson, R. E. (1992). The structure of a *B*-DNA decamer with a central T-A step: CGATTAATCG. *J. Mol. Biol.* **225**, 379-395.
13. Dickerson, R. E. (1999). Helix structure and molecular recognition by *B*-DNA. In *Oxford Handbook of Nucleic Acid Structure* (Neidle, S., ed.), pp. 145-197, Oxford University Press, New York.
14. Dickerson, R. E. (1998). DNA bending: the prevalence of kinkiness and the virtues of normality. *Nucl. Acids Res.* **26**, 1906-1926.
15. Zhurkin, V. B., Lysov, Y. P. & Ivanov, V. I. (1979). Anisotropic flexibility of DNA and the nucleosomal structure. *Nucl. Acids Res.* **6**, 1081-1096.
16. Olson, W. K., Gorin, A. A., Lu, X., Hock, L. M. & Zhurkin, V. B. (1998). DNA sequence-dependent deformability deduced from protein-DNA crystal complexes. *Proc. Natl Acad. Sci. USA,* **95**, 11163-11168.
17. Suzuki, M. & Yagi, N. (1995). Stereochemical basis of DNA bending by transcription factors. *Nucl. Acids Res.* **23**, 2083-2091.
18. Werner, M. H., Gronenborn, A. M. & Clore, G. M. (1996). Intercalation, DNA kinking, and the control of transcription. *Science,* **271**, 778-784.
19. Goodsell, D. S., Kaczor-Grzeskowiak, M. & Dickerson, R. E. (1994). The crystal structure of CCATTAATGG: implications for bending of *B*-DNA at T-A steps. *J. Mol. Biol.* **239**, 79-96.
20. Balendiran, K., Rao, S. T., Sekharudu, C. Y., Zon, G. & Sundaralingam, M. (1995). X-ray structures of the *B*-DNA dodecamer d(CGCGTTAACGCG) with an inverted central tetranucleotide and its netropsin complex. *Acta. Crystallog. sect. D,* **51**, 190-198.
21. Wood, A. A., Nunn, C. M., Trent, J. O. & Neidle, S. (1997). Sequence-dependent crossed helix packing in the crystal structure of the *B*-DNA decamer yields a detailed model for the holliday junction. *J. Mol. Biol.* **269**, 827-841.
22. Spink, N., Nunn, C. M., Bojtechovsky, J., Berman, H. M. & Neidle, S. (1995). Crystal structure of a DNA decamer showing a novel pseudo four-way helix-helix junction. *Proc. Natl Acad. Sci. USA,* **92**, 10767-10771.
23. Liu, J. & Subirana, J. A. (1999). Structure of d(CGCGAATTCGCG) in the presence of Ca^{2+} ions. *J. Biol. Chem.* **274**, 24749-24752.
24. Johansson, E. M., Parkinson, G. & Neidle, S. A. (2000). New crystal form for the dodecamer CGCGAATTCGCG: symmetry effects on sequence-dependent DNA structure. *J. Mol. Biol.* **300**, 551-561.
25. Sines, C. C., McFail-Isom, L., Howerton, S. B., VanDerveer, D. & Williams, L. D. (2000). Cations mediate *B*-DNA conformational heterogeneity. *J. Am. Chem. Soc.* **122**, 11048-11056.
26. Drew, H. R., Wing, R. M., Takano, T., Broka, C., Tanaka, S., Itakura, K. & Dickerson, R. E. (1981). Structure of a *B*-DNA dodecamer conformation and dynamics. *Proc. Natl Acad. Sci. USA,* **78**, 2179-2183.
27. Vlieghe, D., Turkenburg, J. P. & Van Meervelt, L. (1999). *B*-DNA at atomic resolution reveals extended

hydration patterns. *Acta Crystallog. sect. D,* **55**, 1495-1502.
28. Soler-Lopez, M., Malinina, L., Liu, J., Huynh-Dinh, T. & Subirana, J. A. (1999). Water and ions in a high resolution structure of *B*-DNA. *J. Biol. Chem.* **274**, 23683-23686.
29. Minasov, G., Tereshko, V. & Egli, M. (1999). Atomic-resolution crystal structures of *B*-DNA reveal specific influences of divalent metal ions on conformation and packing. *J. Mol. Biol.* **291**, 83-99.
30. Larsen, T. A., Kopka, M. L. & Dickerson, R. E. (1991). Crystal structure analysis of the *B*-DNA dodecamer CGTGAATTCACG. *Biochemistry,* **30**, 4443-4449.
31. Aymani, J., Coll, M., Van Der Marel, G. A., Van Boom, J. H., Wang, J. & Rich, A. (1990). Molecular structure of nicked DNA: a substrate for dna repair enzymes. *Proc. Natl Acad. Sci. USA,* **87**, 2526-2530.
32. DiGabriele, A. D. & Steitz, T. A. (1993). A DNA dodecamer containing an adenine tract crystallizes in a unique lattice and exhibits a new bend. *J. Mol. Biol.* **231**, 1024-1039.
33. Yuan, H., Quintana, J. & Dickerson, R. E. (1992). Alternative structures for alternating Poly(dA-dT) tracts: the structure of the *B*-DNA decamer CGATA-TATCG. *Biochemistry,* **31**, 8009-8021.
34. Yoon, C., Prive, G. G., Goodsell, D. S. & Dickerson, R. E. (1988). Structure of an alternating *B*-DNA helix and its relationship to A-tract DNA. *Proc. Natl Acad. Sci. USA,* **85**, 6332-6336.
35. Shatzky-Schwartz, M., Arbuckle, N. D., Eisenstein, M., Rabinovich, D., Bareket-Samish, A., Haran, T. E. *et al*. (1997). X-ray and solution studies of DNA oligomers and implications for the structural basis of *A*-tract-dependent curvature. *J. Mol. Biol.* **267**, 595-623.
36. Grzeskowiak, K., Yanagi, K., Prive, G. G. & Dickerson, R. E. (1991). The structure of *B*-helical CGATCGATCG and comparison with CCAACGTTGG: the effect of base-pair reversals. *J. Biol. Chem.* **266**, 8861-8883.
37. El Hassan, M. A. & Calladine, C. R. (1996). Propeller-twisting of base-pairs and the conformational mobility of dinucleotide steps in DNA. *J. Mol. Biol.* **259**, 95-103.
38. Dickerson, R. E., Goodsell, D. S. & Neidle, S. (1994). "...the tyranny of the lattice...". *Proc. Natl Acad. Sci. USA,* **91**, 3579-3583.
39. Yanagi, K., Privé, G. C. & Dickerson, R. E. (1991). Analysis of local helix geometry in three *B*-DNA decamers and eight dodecamers. *J. Mol. Biol.* **217**, 201-214.
40. Gorin, A. A., Zhurkin, V. B. & Olson, W. K. (1995). *B*-DNA twisting correlates with base-pair morphology. *J. Mol. Biol.* **247**, 34-48.
41. Prive, G. G., Yanagi, K. & Dickerson, R. E. (1991). Structure of the *B*-DNA decamer of CCAACGTTGG and comparison with the isomorphous decamers CCAAGATTGG and CCAGGCCTGG. *J. Mol. Biol.* **217**, 177-199.
42. Chuprina, V. P. (1987). Anomalous structure and properties of poly (dA).poly(dT). Computer simulation of the polynucleotide structure with the spine of hydration in the minor groove. *Nucl. Acids Res.* **15**, 293-311.
43. Chiu, T. K. & Dickerson, R. E. (2000). 1 Å Crystal structures of the *B*-DNA reveal sequence-specific binding and groove-specific bending of DNA by magnesium and calcium. *J. Mol. Biol.* **301**, 915-945.
44. El Hassan, M. A. & Calladine, C. R. (1997). Conformational characteristics of DNA: empirical classifications and a hypothesis for the conformational behaviour of dinucleotide steps. *Phil. Tans. Roy. Soc. ser. A,* **355**, 43-100.
45. Sarai, A., Mazur, J., Nussinov, R. & Jernigan, R. L. (1989). Sequence dependence of DNA conformational flexibility. *Biochemistry,* **28**, 7842-7849.
46. Barber, A. M. & Zhurkin, V. B. (1990). CAP binding sites reveal pyrimidine-purine pattern characteristic of DNA bending. *J. Biomol. Struct. Dynam.* **8**, 213-232.
47. Rouzina, I. & Bloomfield, V. A. (1998). DNA bending by small, mobile multivalent cations. *Biophys. J.* **74**, 3152-3164.
48. El Hassan, M. A. & Calladine, C. R. (1995). The assessment of the geometry of dinucleotide steps in double-helical DNA: a new local calculation scheme with an appendix. *J. Mol. Biol.* **251**, 648-664.
49. Packer, M. J. & Hunter, C. A. (1998). Sequence-dependent DNA structure: the role of the sugar-phosphate backbone. *J. Mol. Biol.* **280**, 407-420.
50. Juo, S. Z., Chui, T. K., Lieberman, P. M., Baikalov, I., Berk, A. J. & Dickerson, R. E. (1996). How proteins recognize the TATA Box. *J. Mol. Biol.* **261**, 239-254.
51. Otwinowski, Z. (1993). *Oscillation Data Reduction Program 1-56-62*, Daresbury Laboratory, Warrington, UK.
52. Jones, T. A., Zou, J-Y., Cowan, S. W. & Kjeldgaard, M. (1991). Improved methods for building protein models in electron density maps and the location of errors in these models. *Acta Crystallog. sect. A,* **47**, 110-119.
53. Brunger, A. T., Adams, P. D., Clore, G. M., DeLano, W. L., Gros, P., Grosse-Kunstleve, R. W. *et al*. (1998). Crystallography and NMR System: a new software suite for macromolecular structure determination. *Acta. Crystallog. sect. D,* **54**, 905-921.
54. Sheldrick, G. M. & Schneider, T. R. (1997). SHELX-97: high resolution refinement. *Methods Enzymol.* **276**, 319-343.
55. Lavery, R. & Sklenar, H. (1988). The definition of generalised helicoidal parameters and of axis curvature for irregular nucleic acids. *J. Biomol. Struct. Dynam.* **6**, 63-91.
56. Kravlis, P. J. (1991). MOLSCRIPT: a program to produce both detailed and schematic plots of protein structures. *J. Appl. Crystallog.* **24**, 946-950.

Edited by I. Tinoco

(Received 4 June 2001; received in revised form 1 August 2001; accepted 6 August 2001)